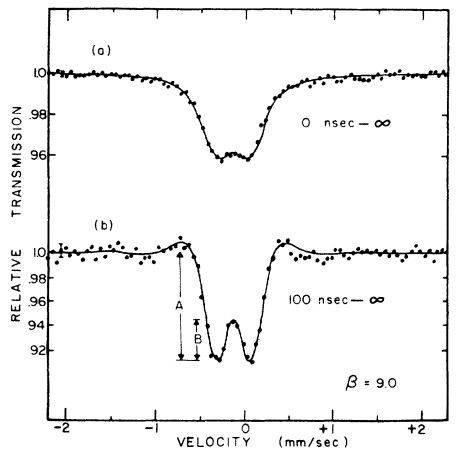

FIG. 3. Regular (a) and coincidence (b) Mössbauer spectra for Pb_2NbFeO_6.

Co^{57}-in-copper source and a Pb_2NbFeO_6 absorber. Figure 3(a) shows the regular Mössbauer results while Fig. 3(b) shows data obtained in delayed coincidence for those nuclei that decay after 100 nsec. The solid lines are computed spectra generated by superimposing two lines separated by 0.38 mm/sec and integrating the time-dependent intensity from 0 to ∞ and 100 nsec to ∞, respectively (numerically ∞ corresponds to 1000 nsec). The value of $\beta = 9.0$ was chosen to fit the observed regular Mössbauer linewidth. Notice that the valley-to-total absorption ratio (B/A) goes from $B/A \approx 0.05$ (regular Mössbauer) to $B/A \approx 0.40$ (coincidence-Mössbauer). In this example it is reasonably clear that two lines are present in the Mössbauer spectrum. If, however, a spectrum contains more lines, e.g., two sets of hyperfine patterns, the enhanced resolution demonstrated here may be essential for extracting the effective field parameters.

*Work supported in part by the U. S. Atomic Energy Commission under Contract No. AT (30-1)-3973, NYO-3973-1.

†Portions taken from a thesis by D.W.H. to be submitted in partial fulfillment of the Ph.D degree.

‡Summer research participant (1968) at the Oak Ridge National Laboratory.

[1]R. E. Holland, F. J. Lynch, G. J. Perlow, and S. S. Hanna, Phys. Rev. Letters 4, 181 (1960).

[2]F. J. Lynch, R. E. Holland, and M. Hamermesh, Phys. Rev. 120, 513 (1960).

[3]C. S. Wu, Y. K. Lee, N. Benczer-Koller, and P. Simms, Phys. Rev. Letters 5, 432 (1960).

[4]S. M. Harris, Phys. Rev. 124, 1178 (1961).

[5]W. Neuwirth, Z. Physik 197, 473 (1966).

[6]S. Margulies and J. R. Ehrman, Nucl. Instr. Methods 12, 131 (1961).

[7]W. Triftshäuser and P. P. Craig, Phys. Rev. Letters 16, 1161 (1966), and Phys. Rev. 162, 274 (1967).

[8]D. W. Hamill and G. R. Hoy, Bull. Am. Phys. Soc. 13, 179 (1968).

[9]K. Abrecht and W. Neuwirth, Z. Physik 203, 420 (1967).

TESTS OF TIME-REVERSAL INVARIANCE OF STRONG INTERACTIONS UTILIZING THE MÖSSBAUER EFFECT*

J. P. Hannon and G. T. Trammell
Physics Department, Rice University, Houston, Texas
(Received 26 July 1968)

The currents induced in the inner electronic shells by a nuclear Mössbauer γ transition gives an $E(L+1)$–$M(L)$ phase difference on the order of 10^{-2}–10^{-3} rad which must be taken into account in the interpretation of experiments designed to detect such phase differences arising from possible failure of T invariance in nuclear interactions.

Recently two groups[1,2] have reported on experiments designed to detect the effect of T-noninvariant nuclear interactions by measuring the angular and polarization dependence of γ-ray absorption or emission using Mössbauer nuclei. Lloyd[3] first pointed out that in a nuclear transition in which a γ ray of mixed multipolarity (e.g., $M1$-$E2$) is emitted (or absorbed) the reduced matrix elements of the current multipole moments which give the amplitudes of the respective radiations (to lower order in e) are in phase (or 180° out of phase) if the strong (and electromagnetic) interactions are T invariant. On the other hand if there is a small T-noninvariant admixture in the interactions then the reduced matrix elements are no longer relatively real. For a mixed $M1$-$E2$ transition,

$$\langle f \| E2 \| i \rangle / \langle f \| M1 \| i \rangle = |\delta| \exp(i\eta), \tag{1}$$

where the deviation of $\eta = \eta_E - \eta_M$ from 0 or π is proportional to the relative admixture of T-noninvariant interaction. Bernstein, Feinberg, and Lee[4] have estimated that under favorable conditions one might obtain an η deviation of the order of 10^{-3}-10^{-2}. Jacobsohn and Henley[5] and Stichel[6] have shown that this will result in the addition of a term proportional to

$$\sin\eta(\hat{e}\cdot\hat{k}\times\hat{j})(\hat{k}\cdot\hat{j})(\hat{e}\cdot\hat{j}) \tag{2}$$

for the probability of emission (or absorption) of a γ ray in the direction $\hat{k}$ with polarization $\hat{e}$, where $\hat{j}$ is the spin of the initial nuclear state. Kistner[1] has attempted to measure the effect of the term (2) in the resonant absorption of the 90-keV Mössbauer γ ray in Ru^{99} and he concludes

$$\eta = \pi - (1.0 \pm 1.7)\times 10^{-3}, \tag{3}$$

whereas Atac, Chrisman, Debrunner, and Frauenfelder[2] have done a similar (emission) experiment utilizing the 73-keV Mössbauer γ ray in Ir^{193} and obtained

$$\eta = (+1.1 \pm 3.8)\times 10^{-3}. \tag{4}$$

Both of the transitions involved are of the mixed $M1$-$E2$ type. One concludes from the experiments that the deviation of the relative phases of the $M1$ and $E2$ radiation from 0 or π which is given by the measurement of (2) is zero to the order of 10^{-3}.

The relative multipole phase difference however does not arise solely from a possible phase difference of the nuclear currents as given by (1), and is then not a direct measure of time reversal. In particular, the $M1$ and $E2$ nuclear transition currents will excite quite different currents in the inner electronic shells (for the cases at hand the K and L shell electrons lie in the near zone, $r < \lambda$). Furthermore, if internal conversion is energetically possible these currents will come mainly from the internal-conversion pole and will be 90° out of phase with the driving nuclear currents. The difference in magnitude of the induced $E2$ and $M1$ conversion currents will cause an extra phase shift ξ between the $E2$ and $M1$ waves emitted from the atom. This extra phase shift, of course, has nothing to do with time reversal.

We have computed ξ for the Ru and Ir Mössbauer transitions and obtained

$$\xi(\mathrm{Ru}) = -6.5\times 10^{-3}, \tag{5}$$

$$\xi(\mathrm{Ir}) = +0.9\times 10^{-3}. \tag{6}$$

Since these phase shifts are of the same order of magnitude as the maximum expected deviation of η from 0 or π due to T noninvariance, the effects of the electronic currents must be taken into account. As we discuss below, these induced electronic currents give quite different effects for emission and absorption experiments.

Coester[7] and Henley and Jacobsohn[8] have previously pointed out that the phase difference in multipole waves emitted or absorbed by a system is indicative of time nonreversibility only to the lowest order in the coupling to the radiation field. Henley and Jacobsohn estimated the effect of the higher order "spoiling terms" for experiments such as these to be $\xi \lesssim 10^{-6}$. However, they considered only polarization effects in the nucleus, which are quite negligible compared with the electronic polarization effects which we have estimated.

Explicitly, if one has a nucleus in an excited state b then the probability per second that it will decay to a state a with the emission of a photon with momentum[9] k_f ($k_f = E_b - E_a$) and polarization $\hat{e}_f$ is $(k_f/4\pi)|T_{ab}(\vec{k}_f, \hat{e}_f)|^2$ where

$$T_{ab}\int \exp(-i\vec{k}_f\cdot\vec{x})\hat{e}_f^{*}\cdot J^{ab}(\vec{x})d\vec{x}, \tag{7}$$

and where

$$J^{ab}(\vec{x}) = \vec{J}^{ab}(\vec{x}) + \int \vec{E}_\nu(\vec{x},\vec{y})[\exp(ik|\vec{y}-\vec{z}|)/|\vec{y}-\vec{z}|]J_\nu^{ab}(\vec{z})d\vec{y}d\vec{z}. \tag{8}$$

In (8) $J_\nu^{ab}(\vec{x})$ is the matrix element of the nuclear current density operator and $\vec{E}_\nu(\vec{x},\vec{y})$ which repre-

sents the susceptibility tensor for the atomic electrons is given (to lowest order in e) by

$$\vec{E}_\nu(\vec{x},\vec{y}) = \sum_p [\vec{j}^{0p}(\vec{x}) j_\nu^{p0}(\vec{y})(E_0 + k + i\epsilon - E_p)^{-1} + j_\nu^{0p}(\vec{y})\vec{j}^{p0}(\vec{x})(E_0 + i\epsilon - k - E_p)^{-1}], \tag{9}$$

where 0 and p refer to the ground and an excited electronic state, respectively, and $j_\nu(\vec{x})$ is the electronic current density operator. To make a spherical-wave expansion of (7)-(9) we utilize the dyad expansions[10,11]

$$\begin{aligned} &\exp(i\vec{k}\cdot\vec{x}) = \sum_{\lambda LM} \vec{Y}_{LM}^{(\lambda)}(\hat{k}_0)^* \vec{A}_{LM}^{(\lambda)}(k\vec{z}), \\ &\exp(ik|\vec{y}-\vec{z}|)/|\vec{y}-\vec{z}| = \sum_{\lambda LM} (ik/4\pi)\vec{B}_{LM}^{(\lambda)}(k\vec{y})\vec{A}_{LM}^{(\lambda)}(k\vec{z})^*, \quad y > z. \end{aligned} \tag{10}$$

In (10) $\lambda = 1, 0, -1$ refer to electric multipole, magnetic multipole, and longitudinal multipole, respectively, the $\vec{A}_{LM}^{(\lambda)}$ are the standing-wave solutions of the vector wave equation, and the $\vec{B}_{LM}^{(\lambda)}$ are the outgoing-wave solutions.[10,11] Substituting the above into (7) we obtain

$$T_{ab} = \sum_{\lambda LM} \hat{e}_f^* \cdot \vec{Y}_{LM}^{(\lambda)}(\hat{k}_f)[1 + E_L^\lambda]\langle a| \int \vec{A}_{LM}^{(\lambda)}(k\vec{x})^* \cdot \vec{J}(\vec{x}) d\vec{x} |b\rangle, \tag{11}$$

where λ is only to be summed over 1 and 0 in (11). E_L^λ represents the effect of the atomic electrons on the outgoing wave emerging from the nucleus (we assume a closed-shell atom so that E_L^λ does not depend on M). If for simplicity we keep only the first sum on the right-hand side of (9) we obtain

$$E_L^\lambda = (ik/4\pi) \int \sum_p \langle 0|\vec{j}(\vec{x})\cdot\vec{A}_{LM}^{(\lambda)}(\vec{x})^*|p\rangle\langle p|B_{LM}^{(\lambda)}(\vec{y})|0\rangle [E_0 + k + ie - E_p]^{-1} d\vec{x} d\vec{y}, \tag{12}$$

where[10,11]

$$B_{LM}^{(0)}(\vec{y}) = -\vec{j}(\vec{y})\cdot\vec{B}_{LM}^{(0)}(k\vec{y}), \tag{13}$$

$$B_{LM}^{(1)}(\vec{y}) = -\vec{j}(\vec{y})\cdot\vec{B}_{LM}^{(1)}(k\vec{y}) + [L/(L+1)]^{1/2}[\rho(\vec{y})\Phi_{LM}(k\vec{y}) - \vec{j}(\vec{y})\cdot\vec{B}_{LM}^{(1)}(k\vec{y})]. \tag{14}$$

In (14) the bracketed term gives the effect of scalar and longitudinal outgoing waves on the atomic electrons. The Feynman diagrams corresponding to (11) are shown in Fig. 1(a).

The real part of E_L^λ gives the effect of the induced electronic currents in (or 180° out of) phase with the nuclear currents, and gives a small correction to the nuclear radiation width, which we may neglect. The principal contribution to the imaginary part of E_L^λ comes from the internal-conversion pole term in (12). Writing $\mathrm{Im}E_L^\lambda = \xi_L^\lambda$ we have from (12)

$$i\xi_L^\lambda \cong (k/4)\sum_p \delta(E_0 + k - E_p)\langle 0| \int \vec{j}(\vec{x})\cdot\vec{A}_{LM}^{(\lambda)}(\vec{x})^*|p\rangle\langle p| \int B_{LM}^{(\lambda)}(\vec{y}) d\vec{y}|0\rangle. \tag{15}$$

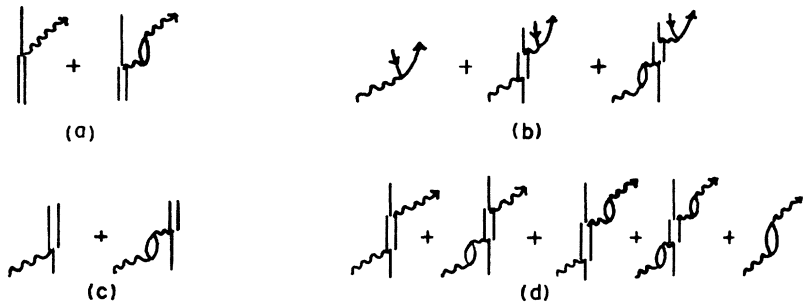

FIG. 1. Feynman diagrams for the emission, absorption, and scattering amplitudes. The external wavy lines represent the incident and scattered photons, and the internal lines represent virtual photon exchange. The single vertical lines represent the ground states of the nucleus, and the double lines the excited states. The "bubbles" represent an excited electron with a hole in a normally filled electronic level.

For the inner electron shells we shall have $kr \ll 1$ for which the spherical Hankel functions in $B_{LM}^{(\lambda)}$ are purely imaginary, $B_{LM}^{\lambda}(r) \sim i(kr)^{-L-1}$, whereas the spherical Bessel functions which enter in A_{LM}^{λ} are real.

The $B_{LM}^{(\lambda)}$ matrix element appearing in (15) is that which is involved in internal-conversion coefficient computations and we have taken the tabulated values given by Rose[12] and Band, Listengarten, and Sliv.[13] The $A_{LM}^{(\lambda)}$ matrix elements (which are those involved in photoelectric cross sections) were computed using Dirac Coulomb wave functions. The results are given in (5) and (6). We might mention that the K-shell conversion channel is closed for the 73-keV Ir^{193} transition and (6) represents the contribution of the L shell. We give a fuller discussion of (15) in a forthcoming paper on Mössbauer γ-ray optics[14]; we mention here that (15) is of order of magnitude $(k/4)$ times the geometric mean of the internal conversion coefficient and the partial cross section for (λ, L) photoelectron emission, and is directly related to the interference term in the cross section of the processes indicated in Fig. 1(b).

The emission amplitude T_{ab} may now be written

$$T_{01} = \sum_{\lambda LM} (-1)^{M} \hat{e}_f^{*} \cdot \vec{Y}_{LM}^{(\lambda)}(\hat{k}_f) \exp[i(\eta_L^{\lambda} + \xi_L^{\lambda})] \langle \chi_L^{\lambda} | C(j_1 L j_0; m_1 - M m_0), \tag{16}$$

where we have taken $|b\rangle = |\alpha_1 j_1 m_1\rangle$, $|a\rangle = |\alpha_0 j_0 m_0\rangle$ to represent the initial and final nuclear states which are assumed to be states of good parity, $\vec{J}^2$, and J_z, and where

$$\langle \alpha_0 j_0 m_0 | \int \vec{A}_{LM}^{(\lambda)}(\vec{x})^{*} \cdot \vec{J}(\vec{x}) d\vec{x} | \alpha_1 j_1 m_1 \rangle = (-1)^{M} \langle \chi_L^{\lambda} | \exp(i\eta_L^{\lambda}) C(j_1 L j_0; m_1 - M m_0). \tag{17}$$

In a similar fashion we have for the amplitude for photon absorption leading to nuclear excitation [Fig. 1(c)]

$$T_{10} = \sum_{\lambda LM} (-1)^{M} \langle \chi_L^{\lambda} | C(j_1 L j_0; m_1 - M m_0) \exp[i(\xi_L^{\lambda} - \eta_L^{\lambda})] \vec{Y}_{LM}^{(\lambda)}(\hat{k}_0)^{*} \cdot \hat{e}_0. \tag{18}$$

From (16) and (18) we obtain for the scattering amplitude proceeding via nuclear excitation [Fig. 1(d)]

$$S_{f0} = \sum_{\lambda LM} \sum_{\lambda' L' M'} \hat{e}_f^{*} \cdot \vec{Y}_{LM}^{(\lambda)}(\hat{k}_f) \exp[i(\xi_L^{\lambda} + \eta_L^{\lambda})] \langle \chi_L^{\lambda} | C(j_1 L j_0; m_1 - M m_0) \times \langle \chi_{L'}^{\lambda'} | C(j_1 L' j_0; m_1 - M' m_0') \exp[i(\xi_{L'}^{\lambda'} - \eta_{L'}^{\lambda'})] \vec{Y}_{L'M'}^{(\lambda')}(\hat{k}_0)^{*} \cdot \hat{e}_0 R^{-1}, \tag{19}$$

where $R = E_0 + k_0 - (E_1 - i\Gamma_{1/2})$ is the nuclear resonance denominator.

It is straightforward to verify that if $\eta_L^{\lambda} - \eta_{L'}^{\lambda'} = 0, \pi$, then the emission and absorption amplitudes (16) and (18) are equal under time reversal (to an overall phase factor), and hence the scattering amplitude (19) is also invariant under time reversal (time reversibility however does not put any restrictions on the ξ_L^{λ}). Under time reversal, the emission amplitude (16) becomes

$$\begin{aligned} T_{01}'(\hat{e}_0, -k_0) &= \hat{e}_0 \cdot \sum_{\lambda LM} \vec{Y}_{LM}^{(\lambda)}(-\hat{k}_0) \exp i\xi_L^{\lambda} (-1)^{(j_1 + j_0 - m_1 - m_0 + 1)} \langle \alpha_0 j_0 - m_0 | \vec{A}_{LM}^{(\lambda)*} \cdot \vec{J} | \alpha_1 j_1 - m_1 \rangle \\ &= \hat{e}_0 \cdot \sum_{\lambda LM} (-1)^{(L + M + j_1 + j_0 - m_1 - m_0)} \vec{Y}_{L-M}^{(\lambda)}(\hat{k}_0)^{*} \\ &\quad \times \exp i\xi_L^{\lambda} (-1)^{M} \langle \chi_L^{\lambda} | \exp i\eta_L^{\lambda} C(j_1 L j_0; -m_1 M - m_0) \\ &= \sum_{\lambda LM} (-1)^{M} \langle \chi_L^{\lambda} | C(j_1 L j_0; m_1 - M m_0) \exp[i(\xi_L^{\lambda} + \eta_L^{\lambda})] \vec{Y}_{LM}^{(\lambda)}(\hat{k}_0)^{*} \cdot \hat{e}_0. \end{aligned} \tag{20}$$

Comparing (20) and (18), we see that $T_{01}'(\hat{e}_0, -\vec{k}_0) = T_{10}(\hat{e}_0, \vec{k}_0)$ (to an overall phase factor) only if $\eta_{L'}^{\lambda'} - \eta_L^{\lambda} = 0, \pi$, but the ξ_L^{λ} can be quite arbitrary since they enter both expressions with the same sign.

For further discussion purposes we shall consider the case where the overlap of the resonances cor-

responding to the transitions between the various Zeeman sublevels of the two nuclear levels can be neglected. In Eqs. (16)-(19) then we consider a particular $m_0, m_1, M = m_1 - m_0$, term. We also consider the common case in which only one electric multipole, EL, and one magnetic multipole, ML', γ ray is allowed by the transition (e.g., $M1$-$E2$). Now by definition[15]

$$\vec{Y}_{LM}^{\,E}(\hat{r}) \equiv \vec{Y}_{LM}^{\,(1)}(\hat{r}) = [L(L+1)]^{-\frac{1}{2}} r \nabla Y_{LM}(\hat{r}) \equiv (Y_\theta^{\,E}\hat{\theta} + iY_\varphi^{\,E}\hat{\varphi}) \exp(iM\varphi),$$

$$\vec{Y}_{L'M}^{\,M}(\hat{r}) \equiv \vec{Y}_{L'M}^{\,(0)}(\hat{r}) = -i[L'(L'+1)]^{-\frac{1}{2}} \hat{r} \times \nabla Y_{L'M}(\hat{r}) \equiv (Y_\theta^{\,M}\hat{\theta} + iY_\varphi^{\,M}\hat{\varphi}) \exp(iM\varphi), \tag{21}$$

where $Y_{\theta,\varphi}^{\,E}, Y_{\theta,\varphi}^{\,M}$ are all real. We now have for the emission amplitude (16) and for the nuclear excitation amplitude (18)

$$T_{01} = \exp(iM\varphi)\hat{e}_f^{\,*} \sum_{\lambda=E,M} (A_\theta^{\,\lambda}\hat{\theta} + iA_\varphi^{\,\lambda}\hat{\varphi}) \exp(i\psi_\lambda), \tag{22}$$

$$T_{10} = \exp(-iM\varphi)\hat{e}_0^{\,*} \sum_{\lambda=E,M} (A_\theta^{\,\lambda}\hat{\theta} - iA_\varphi^{\,\lambda}\hat{\varphi}) \exp(i\psi_\lambda'), \tag{23}$$

where $A_{\theta,\varphi}^{\,\lambda}$ are the functions $Y_{\theta,\varphi}^{\,\lambda}$ of (21) multiplied by their appropriate reduced matrix element (absolute value) and Wigner coefficient, and where $\psi_\lambda = \xi_\lambda + \eta_\lambda, \psi_\lambda' = \xi_\lambda - \eta_\lambda$. From (22) we have for the emission probability [to terms linear in $\sin(\psi_E - \psi_M)$]

$$|T_{01}|^2 = (A_\theta^{\,E} + A_\theta^{\,M})^2(\hat{e}\cdot\hat{\theta})^2 + (A_\varphi^{\,E} + A_\varphi^{\,M})^2(\hat{e}\cdot\varphi)^2 - 2\sin(\psi_E - \psi_M)(A_\theta^{\,E}A_\varphi^{\,M} - A_\varphi^{\,E}A_\theta^{\,M})\hat{e}\cdot\hat{\theta}\hat{e}\cdot\hat{\varphi}, \tag{24}$$

and $|T_{10}|^2$, proportional to the nuclear excitation cross section, is

$$|T_{10}|^2 = (A_\theta^{\,E} + A_\theta^{\,M})^2(\hat{e}\cdot\hat{\theta})^2 + (A_\varphi^{\,E} + A_\varphi^{\,M})^2(\hat{e}\cdot\hat{\varphi})^2 + 2\sin(\psi_E' - \psi_M')(A_\theta^{\,E}A_\varphi^{\,M} - A_\varphi^{\,E}A_\theta^{\,M})\hat{e}\cdot\hat{\theta}\hat{e}\cdot\hat{\varphi}. \tag{25}$$

It is the $\hat{e}\cdot\hat{\theta}\hat{e}\cdot\hat{\varphi}$ term in (24) and (25) which is responsible for rotating the axis of the polarization ellipse away from the z axis.

Thus we see that in an emission experiment the measurement gives $\eta' = \xi_E + \eta_E - (\xi_M + \eta_M)$ and one must correct the measurements by calculation of $\xi_E - \xi_M$ (which as we have seen $\sim 10^{-3}$) to deduce values for $\eta_E - \eta_M$. Thus in the results of the experiment of Ref. 2, η should be replaced by η' on the left-hand side of Eq. (2). Assuming $\eta \equiv 0$, the calculated value of $\eta' = +0.9 \times 10^{-3}$ is in good agreement in both sign and magnitude with the measured value of $(+1.1 \pm 3.8) \times 10^{-3}$.

Similarly, in an absorption experiment in which the nucleus is excited the measurement gives $\xi_E - \eta_E - (\xi_M - \eta_M)$ which requires a similar correction to obtain $\eta_E - \eta_M$. However it is very important that for the total absorption cross section the $\hat{e}\cdot\hat{\theta}\hat{e}\cdot\hat{\varphi}$ term is independent of $\xi_M - \xi_E$, being proportional only to $\eta_E - \eta_M$, and thus furnishing a direct measurement of T-noninvariant interactions. The rotation of the polarization ellipse for the absorption cross section is only given by (25) for those processes which definitely occur via nuclear excitation, e.g., inelastic scattering for which the initial and final nuclear Zeeman states are different. In the total cross section, however, there appear interference terms between coherent processes, the most important of which is that of Fig. 1(b) representing the interference between photoelectric absorption and internal conversion following nuclear excitation, and these interference terms cancel out the ξ dependence of the $\hat{e}\cdot\hat{\theta}\hat{e}\cdot\hat{\varphi}$ terms for the processes taking place via nuclear excitation. This is most easily seen by using expressions (19), (22), and (23) and the optical theorem to compute the total cross section. The result is

$$\begin{aligned}\sigma(\hat{e}, \vec{k}) = 4\pi\lambda\Gamma/2[\Delta^2 + (\Gamma/2)^2]^{-1}\{&(A_\theta^{\,E} + A_\theta^{\,M})^2(\hat{e}\cdot\hat{\theta})^2 + (A_\varphi^{\,E} + A_\varphi^{\,M})^2(\hat{e}\cdot\hat{\varphi})^2 + 2\sin(\eta_E - \eta_M) \\ &\times (A_\varphi^{\,E}A_\theta^{\,M} - A_\theta^{\,E}A_\varphi^{\,M})\hat{e}\cdot\hat{\theta}\hat{e}\cdot\hat{\varphi} - (4\Delta/\Gamma)[(\hat{e}\cdot\hat{\theta})^2(A_\theta^{\,E} + A_\theta^{\,M})(\xi_E A_\theta^{\,E} + \xi_M A_\theta^{\,M}) \\ &+ (\hat{e}\cdot\hat{\varphi})^2(A_\varphi^{\,E} + A_\varphi^{\,M})(\xi_E A_\varphi^{\,E} + \xi_M A_\varphi^{\,M})]\} + \sigma_{\mathrm{el}},\end{aligned} \tag{26}$$

where $\Delta = E_0 + k - E_1$ and σ_{el} is the total cross section of the atomic electrons for the incident γ ray. It is seen that the $\hat{e}\cdot\hat{\theta}\hat{e}\cdot\hat{\varphi}$ term in the total cross section is directly proportional to the T-noninvariant interaction.

Thus for sufficiently thin films, an absorption experiment will give a direct measurement of T noninvariance. However, even for a film as thin as in Kistner's experiment for which the absorption at resonance is only about 3%, multiple scattering effects (such as Faraday rotations) must be considered. In Ref. 14, we give a detailed treatment of the Kistner experiment using the dynamical theory of γ-ray optics. Here we will only state the final results: The intensity of the Mössbauer wave transmitted through the polarizing medium A and the absorbing medium B will contain an "electronic screening" term, E, proportional to $\xi_E - \xi_M$ which has the same symmetry properties[1] as the T-noninvariant $\sin\eta$ term, T (i.e., E and T change sign when the field is reversed in B, and they change sign with a change in sign of $M = m_1 - m_0$). However, E and T have a different dependence on the thickness of B and upon the resonance denominator (T has a linear dependence and E a quadratic dependence), and the two effects can be determined independently. More explicitly, the dynamical theory gives, in place of Kistner's Eq. (3),[1] the equations (at resonance)

$$\Delta I_+ = A_{(+)}B_{(+)}^{(2)}[0.58 + 4.1(\xi_E - \xi_M)] - A_{(+)}B_{(+)}^{(1)}[1.9\sin\eta]$$
$$\Delta I_- = A_{(-)}B_{(-)}^{(2)}[0.58 - 4.1(\xi_E - \xi_M)] + A_{(-)}B_{(-)}^{(1)}[1.9\sin\eta], \qquad (27)$$

where the subscripts $\pm$ refer to the source being in resonance with the $M = \pm 1, \mp\frac{5}{2} \rightarrow \mp\frac{3}{2}$ Ru^{99} transitions. The factors with opposite subscripts can be taken equal to order 10^{-2}. The factor $B(2)$ is quadratic in the thickness of the absorbing medium B and the resonance denominator, while $B(1)$ is linear. The first term, $0.58B(2)$, gives the Faraday rotation effects, and the second and third terms give E and T, respectively. The factors $A_{(\pm)}$ are proportional to the degree of polarization obtained in the polarizing medium A.

For emphasis, we note again that by Doppler shifting or by using two absorbers B and B' which differ in the concentration-thickness of Mössbauer atoms, Eq. (27) will determine both $\sin\eta$ and $\xi_E - \xi_M$.[16]

Kistner's data are not sufficient to solve for both quantities, but if it is assumed that there is no T noninvariance (i.e., $\sin\eta = 0$), then Kistner's measurements give

$$\langle \xi_E - \xi_M \rangle = (-8.6 \pm 10.2) \times 10^{-3}, \qquad (28)$$

where the weighted average of the two runs has been taken. The calculated value of -6.5×10^{-3} again agrees well in both sign and magnitude with experiment.

---

*Work supported in part by National Aeronautics and Space Administration and by U. S. Atomic Energy Commission.

[1]O. C. Kistner, Phys. Rev. Letters 19, 872 (1967).
[2]M. Atac, B. Chrisman, P. Debrunner, and H. Frauenfelder, Phys. Rev. Letters 20, 691 (1968).
[3]S. P. Lloyd, Phys. Rev. 83, 716 (1951).
[4]J. Bernstein, G. Feinberg, and T. D. Lee, Phys. Rev. 139, B1650 (1965).
[5]B. A. Jacobsohn and E. M. Henley, Phys. Rev. 113, 234 (1959).
[6]P. Stichel, Z. Physik 150, 264 (1958).
[7]F. Coester, Phys. Rev. 89, 619 (1953).
[8]E. M. Henley and B. A. Jacobsohn, Phys. Rev. Letters 16, 706 (1966).
[9]Throughout this paper, we take $\hbar = c = 1$.
[10]See, for example, the article by M. E. Rose, in Alpha-, Beta-, and Gamma-Ray Spectroscopy, edited by K. Siegbahn (North-Holland Publishing Company, Amsterdam, The Netherlands, 1965), Vol. II, Chap. XVI, p. 887.
[11]A. I. Akhiezer and V. B. Berestetskii, Quantum Electrodynamics (Interscience Publishers, Inc., New York, 1965), pp. 27-29, 537-541.
[12]M. E. Rose, Internal Conversion Coefficients (North-Holland Publishing Company, Amsterdam, The Netherlands, 1958).
[13]I. M. Band, M. A. Listengarten, and L. A. Sliv, in Alpha-, Beta-, and Gamma-Ray Spectroscopy, edited by K. Siegbahn (North-Holland Publishing Company, Amsterdam, The Netherlands, 1965), Vol. II, pp. 1673-1680.

[14]J. P. Hannon and G. T. Trammell, to be published.
[15]Ref. 11, pp. 27-29. We also note that the superscript M on the $Y_{\theta\varphi}{}^{M}, A_{\theta\varphi}{}^{M}$ functions refer to "magnetic multpole," and should not be confused with $M = m_1 - m_0$.
[16]We wish to acknowledge a helpful conversation with Dr. B. Chrisman and Dr. P. Debrunner on this point.

INSTABILITY MODES PRIOR TO MELTING*

B. J. Alder, W. R. Gardner,† J. K. Hoffer, N. E. Phillips, and D. A. Young
Lawrence Radiation Laboratory, Livermore, California, and Inorganic Materials Research Division, and Department of Chemistry, University of California, Berkeley, California 94720
(Received 26 July 1968)

An unexpected rise in the constant-volume heat capacity of bcc He^4 is observed in the 0.02°K interval below the discontinuity at melting, giving thermodynamic evidence for the appearance of new modes of motion associated with the break up of the crystal. The appearance of slipping motion in molecular-dynamics computer experiments with hard-particle systems allows the nature of these instabilities to be examined.

Melting usually appears in thermodynamic measurements as a sharp transition at a density that is well approximated by the empirical Lindemann law.[1] At the melting density a process which can break up the long-range order of the crystal and cause the disappearance of low-frequency shear waves in the fluid becomes sufficiently probable. It is, therefore, natural to propose that at the melting point the crystal becomes unstable to a long-wavelength transverse shear mode.[2] The problem associated with any instability criterion is that it can apply only at a point beyond the thermodynamic stability limit and lead to van der Waals–like behavior as, for example, in the infinite compressibility criterion. Furthermore, it is not possible to identify the stable phase that the instability leads to; it could be another crystal structure. Nevertheless, the difference in the ability to support a long-wavelength transverse mode is a general way to distinguish between a solid and a fluid; the frequently used alternative of the degree of order does not distinguish between a solid and a fluid in two dimensions.[3]

The lack of experimental evidence in favor of associating instabilities with melting is not surprising in view of the difficulty of detecting the appearance of one or a few highly cooperative low-frequency modes, particularly by measurement of thermodynamic properties which are usually dominated by the more abundant high-frequency modes. In helium, however, the melting temperature is so low that the high-frequency modes are not yet fully excited and the heat capacity contribution of an excitation appearing just prior to melting is relatively more significant. Furthermore, it should be particularly prominent in the bcc phase because the transverse (110) mode is well known to be of low-frequency.[4]

We have measured the heat capacity C_V of He^4 at a number of densities in the bcc and low-density hcp phases. The samples were contained in a pressure cell that was sealed by a remotely-operated valve located at the cell itself. Problems associated with the use of a plug of solid He to seal the filling tube were thus avoided. A typical result for one sample passing through the bcc phase is shown in Fig. 1.

The expected discontinuous increase of C_V at the melting temperature of the bcc phase is preceded by a rapid but smooth increase beginning 0.02°K lower, which is accompanied by an increase in the thermal relaxation time of the sample. This behavior is independent of the thermal history of the sample and was even observed when the heat-capacity points were taken with decreasing temperature (by balancing a negative heat leak with a power input that was interrupted to produce a decrease in sample temperature). Edwards and Pandorf[5] observed a similar effect but attributed it to pressure gradients in their sample and did not report their data in this region. Their cell was filled with sintered copper powder leaving an average pore diameter of 10 μ, and they observed other effects indicative of pressure gradients. However, the other effects disappeared after a half-hour anneal but the premelting "tail" in C_V did not. In the measurements reported here there is no reason to expect pressure gradients in the sample and no effects attributable to them were observed. We have